Smart Structures and Systems, *Vol. 33, No. 3 (2024) 201-215*
https://doi.org/10.12989/sss.2024.33.3.201

A combined spline chirplet transform and local maximum synchrosqueezing technique for structural instantaneous frequency identification

Ping-Ping Yuan*[1], Zhou-Jie Zhao [1a], Ya Liu [2b] and Zhong-Xiang Shen [3c]

[1] *School of Civil Engineering and Architecture, Jiangsu University of Science and Technology, Zhenjiang, 212100, Jiangsu, China*
[2] *The First Construction Engineering Company Ltd. of China Construction Second Engineering Bureau, Beijing, 100176, China*
[3] *School of Naval Architecture and Ocean Engineering, Jiangsu University of Science and Technology, Zhenjiang, 212100, Jiangsu, China*

(*Received April 7, 2023, Revised December 22, 2023, Accepted January 26, 2024*)

Abstract. Spline chirplet transform and local maximum synchrosqueezing are introduced to present a novel structural instantaneous frequency (IF) identification method named local maximum synchrosqueezing spline chirplet transform (LMSSSCT). Namely spline chirplet transform (SCT), a transform is firstly introduced based on classic chirplet transform and spline interpolated kernel function. Applying SCT in association with local maximum synchrosqueezing, the LMSSSCT is then proposed. The index of accuracy and Rényi entropy show that LMSSSCT outperforms the other time-frequency analysis (TFA) methods in processing analytical signals, especially in the presence of noise. Numerical examples of a Duffing nonlinear system with single degree of freedom and a two-layer shear frame structure with time-varying stiffness are used to verify the effectiveness of structural IF identification. Moreover, a nonlinear supported beam structure test is conducted and the LMSSSCT is utilized for structural IF identification. Numerical simulation and experimental results demonstrate that the presented LMSSSCT can effectively identify the IFs of nonlinear structures and time-varying structures with good accuracy and stability.

Keywords: instantaneous frequency; local maximum synchrosqueezing; local maximum synchrosqueezing spline chirplet transform; spline chirplet transform

1. Introduction

Affected by various factors such as loads, environmental changes and material aging, civil engineering structures are generally time-varying and nonlinear structural systems during their service life, and their vibration response signals are typically non-stationary (Liu *et al*. 2018a, b, Wang *et al*. 2020). As an effective tool for processing non-stationary signals, TFA technology is widely used in signal processing, mechanical fault diagnosis, seismic exploration, engineering structural instantaneous parameters identification and other fields. However, traditional TFA methods cannot obtain high time-frequency resolution when dealing with complex signals. To improve the time-frequency energy concentration of signals, relevant scholars have upgraded and improved the traditional TFA methods from the points of self-adaptation, parameterization, and post-processing, and put forward a series of novel methods.

The energy of ideal time-frequency ridge should be more concentrated, and the readability should also be better. However, how to obtain clear time-frequency diagram or ridge of engineering measured signal is still a problem to be solved. Therefore, Daubechies *et al*. (2011) creatively proposed an empirical mode decomposition-like tool named synchrosqueezed wavelet transform based on wavelet transform and synchrosqueezing transform (SST), which can effectively improve the aggregation of time-frequency distributed energy by squeezing the energy near the ridge of wavelet transform. Liu *et al*. (2019) effectively identified IF of time-varying structures by means of extended analytical mode decomposition method, a recursive Hilbert transform and a zoom synchrosqueezing wavelet transform. Sony and Sadhu (2020) conducted synchrosqueezing transform-based identification of time-varying structural systems using multi-sensor data. Enhanced by extended analytical mode decomposition method, Wang *et al*. (2013) proposed a synchrosqueezed wavelet transform method for dynamic signal reconstruction. Combining generalized S-transform with SST, Chen *et al*. (2017) proposed synchrosqueezing generalized S-transform to meet the needs of high-resolution seismic signal processing and interpretation. The synchrosqueezing generalized S-transform method can squeeze and reconstruct the complex coefficient spectra of generalized S-transform results along the frequency direction so that the energy distributions on the time-frequency spectra are concentrated around the real IF of the signal. Pham and Meignen (2017) put forward a high-order synchrosqueezing transform method for multi-component signals analysis. Yu *et al*. (2018) further proposed multi-synchrosqueezing transform for signal processing and parameters identification. Combining a new form of improved generalized S-transform and a multi-synchrosqueezing operation, Yuan *et al*. (2021) conducted

*Corresponding author, Ph.D., Associate Professor,
E-mail: yuanpingping@just.edu.cn
[a] Graduate Student, E-mail: 3435519317@qq.com
[b] Structural Engineer, E-mail: 549209246@qq.com
[c] Ph.D., E-mail: zhongxiang-shen@just.edu.cn

ISSN: 1738-1584 (Print), 1738-1991 (Online)

structural IF extraction based on improved multi-synchrosqueezing generalized S-transform.

Inspired by SST, Yu *et al*. (2017) creatively put forward synchroextracting transform (SET) based on short-time Fourier transform. This algorithm only extracts the ridge of time-frequency distribution, and eliminates other divergent energy. So, it can effectively improve the energy concentration and enhance the resolution of IF. Furthermore, many scholars have conducted in-depth exploration of this method. Combining different TFA methods with SET (Chen *et al*. 2019, Shi *et al*. 2021, Liu and Xiang 2018, Xin *et al*. 2019, Sahu *et al*. 2020, Chen *et al*. 2019, Li *et al*. 2020a, Yuan *et al*. 2022), various modified algorithms have been carried out and the theoretical framework of SET has been gradually improved. For example, Liu and Xiang (2018) proposed kernel regression residual decomposition-based SET to detect faults in mechanical systems. Xin *et al*. (2019) conducted time-varying system identification by enhanced empirical wavelet transform based on SET. Chen *et al*. (2019) further introduced an upgraded SET, namely ameliorated synchroextracting transform, to deal with fast time-varying and strong frequency modulated signals for TFA. Li *et al*. (2022a) summarily compared SST and SET, and verified the accuracy of SET for processing non-stationary signals. To get higher IF identification accuracy, Yuan *et al*. (2022) proposed an improved time-frequency analysis method for structural IF identification based on generalized S-transform and synchroextracting transform. Furthermore, Yuan *et al*. (2021) put forward structural instantaneous frequency extraction based on improved multi-synchrosqueezing generalized S-transform.

As an efficient TFA method for processing linear frequency modulated signals, chirplet transform is widely used by many scholars. However, the linear chirplet transform and its variants in classic forms cannot be used to reliably analyze nonlinear frequency modulated signals. To adapt chirplet transform to signals with nonlinear IF, Yang *et al*. (2011, 2013, 2014) proposed a generalized parametric chirplet TFA method, which improved the identification accuracy of IF through different kernel function fitting. To reduce the workload caused by kernel function fitting, Yu and Zhou (2016) creatively introduced rotation factors and proposed the generalized linear chirplet transform, which effectively improved the computational efficiency. Guan *et al*. (2019) put forward velocity synchronous linear chirplet transform in combination with a kurtosis-guided method. Furthermore, Guan and Feng (2022) proposed an adaptive linear chirplet transform for analyzing signals with crossing frequency trajectories. By introducing a kernel function that can be modulated with time and frequency, Li *et al*. (2020b) originally proposed the scale-based chirplet transform. Combining SET and chirplet transform, Zhu *et al*. (2019) further proposed an IF identification method based on synchroextracting chirplet transform, and realized signal reconstruction. Yu *et al*. (2019) further proposed an energy-concentrated TFA tool called local maximum synchrosqueezing transform. Based on the former research, He *et al*. (2021) proposed an effective tool named local maximum synchrosqueezing chirplet transform for strongly nonstationary signals of gas turbine. Based on the classical chirplet transform and the second-order synchroextracting transform, Meng *et al*. (2021) proposed general synchroextracting chirplet transform and applied it to rotor rub-impact fault diagnosis.

To further improve energy aggregation, in this paper, a novel structural IF identification method is proposed, namely LMSSSCT. At first, a transform named SCT is introduced based on the classic chirplet transform and spline interpolated kernel function. Then, to further improve time-frequency resolution, the local maximum synchrosqueezing is introduced, and the so-called LMSSSCT is proposed. The superior accuracy and robustness against noise of this method are verified by IF identification of both single component signal and multi-component signal. In terms of numerical structural simulation, the IF identifications of a Duffing nonlinear system and a two-layer time-varying stiffness shear frame structure are conducted. Furthermore, in order to validate the effectiveness of this method for practical structures, in the experimental aspect, the nonlinear supported beam structure test is designed and carried out. The IF identified by LMSSSCT is compared with the IF identified by SST, SET and theoretical frequency to verify the effectiveness and superiority of the proposed method. At last, this paper ends up with some conclusions and lists some recommendations for future work.

2. Theoretical basis

2.1 SCT

The chirplet transform introduces the concept of frequency-rotate operator and frequency-shift operator to process linear frequency modulated signals by depicting the kernel function with linear frequency modulated parameters. For a frequency-modulated time varying signal $s(t)$, its chirplet transform CT_s at time t_0 is

$$CT_s(t_0,\omega,\alpha;\sigma) = \int_{-\infty}^{+\infty} z(t)\ \psi(t,t_0,\alpha,\sigma)\, exp(-j\omega t)dt \tag{1}$$

where, $z(t)$ is the analytical signal of $s(t)$, that is $z(t) = s(t) + jH[s(t)]$. $\psi(t,t_0,\alpha,\sigma)$ represents a complex window function, which is given by the following formula

$$\psi(t,t_0,\alpha,\sigma) = w_\sigma(t-t_0)\, exp(-j\alpha(t-t_0)^2/2) \tag{2}$$

where, w_σ stands for a nonnegative symmetric normalized Gaussian window function which is defined as

$$w_\sigma(t) = \frac{1}{\sqrt{2\pi}\sigma} exp\left(-\frac{1}{2}\left(\frac{t}{\sigma}\right)^2\right) \tag{3}$$

in which, σ stands for standard deviation of Gaussian window.

According to the definition formula, the chirplet transform can be seen as a short-time Fourier transform obtained by multiplying the analytical signal and the window function. It is essentially Fourier transform of the

frequency modulated windowed signal. Therefore, the definition of the chirplet transform can also be expressed as

$$\begin{aligned} &CT_s(t_0,\omega,\alpha;\sigma) \\ &= A(t_0,\alpha)\int_{-\infty}^{+\infty}\bar{z}(t)\,w_\sigma(t-t_0)\,exp(-j\omega t)dt \\ &\bar{z}(t) = z(t)\Phi^R(t,\alpha)\Phi^S(t,t_0,\alpha) \\ &\Phi^R(t,\alpha) = exp(-j\alpha t^2/2) \\ &\Phi^s(t,t_0,\alpha) = exp(-j\alpha t_0 t) \\ &A(t_0,\alpha) = exp(-j\alpha t_0^2/2) \end{aligned} \tag{4}$$

where, $\Phi^R(t,\alpha)$ is frequency-rotate operator, $\Phi^S(t,t_0,\alpha)$ represents frequency-shift operator. The frequency-rotate operator is to rotate analytical signal $z(t)$ in the time-frequency plane by degree of θ, and $tan(\theta) = -\alpha$; while the frequency-shift operator is to translate frequency component at t_0 upwards by αt_0; $A(t_0,\alpha)$ is a plural and $|A(t_0,\alpha)| = 1$.

When the IF of the signal is a nonlinear time-varying function, the traditional chirplet transform is no longer applicable on entire time domain, and it cannot even estimate the IF trajectory. To solve the problem, this paper introduces spline interpolated function as chirplet transform kernel function to process nonlinear frequency modulated signal, that is, the SCT

$$\begin{aligned} &SCT_s(t_0,\omega,Q;\sigma) \qquad t_0 \in (t_i,t_{i+1}) \\ &= \int_{-\infty}^{+\infty}\bar{z}(t)\,w(t-t_0,\omega)\,exp(-j\omega t)dt \\ &\bar{z}(t) = z(t)\Phi^R(t,Q)\Phi^S(t,t_0,Q) \\ &\Phi^R(t,Q) = exp\left(-j\sum_{k=1}^{n}\frac{q_k^i}{k}(t-t_i)^k + \gamma_i\right) \\ &\Phi^S(t,t_0,Q) = exp\left(j\sum_{k=1}^{n}q_k^i\,(t_0-t_i)^{k-1}t\right) \end{aligned} \tag{5}$$

where, $\Phi^R(t,Q)$ and $\Phi^S(t,t_0,Q)$ are frequency-rotate operator and frequency-shift operator, respectively. $Q(i,k) = q_k^i$ represents the polynomial coefficient matrix of spline interpolated kernel function. The coefficient γ_i meets the following condition

$$\gamma_i - \gamma_{i+1} = \sum_{k=1}^{n}\frac{q_k^{i+1}}{k}(t_i - t_{i+1})^k \tag{6}$$

with $\gamma_1 = 0$.

The spline parameters of SCT can be obtained by interpolating and fitting the frequency trends which are firstly gained by chirplet transform and local maximum synchrosqueezing.

2.2 LMSSSCT

In order to further improve the time-frequency aggregation and resolution of the signal, this paper introduces local maximum synchrosqueezing technique to compress the SCT results. LMSSSCT retains the coefficient on the time-frequency ridge and eliminate other divergent energy so as to achieve the purpose of focusing time-frequency energy and improving resolution. LMSSSCT gathers the diffused time-frequency energy by a novel frequency reassignment operator. The expression of the LMSSSCT can be written as

$$LSCT_s(t_0,\omega) = \int_{-\infty}^{+\infty}SCT_s(t_0,\omega)\delta(\xi - \widehat{\omega}(t_0,\omega))d\omega \tag{7}$$

where, SCT_s stands for SCT of signal $s(t)$, δ is Dirac function, the two-dimensional frequency estimate $\widehat{\omega}(t_0,\omega)$ can be obtained from the following equation

$$\widehat{\omega}(t_0,\omega) = \begin{cases} \arg\max\limits_{\omega} |SCT_S(t_0,\omega), \\ \omega \in [\omega-\Delta,\omega+\Delta]|, SCT_S(t_0,\omega)| \neq 0 \\ 0, \;\; SCT_S(t_0,\omega)| = 0 \end{cases} \tag{8}$$

where, the Δ value should satisfy the condition: $\Delta < \Delta\omega/2$. It can be seen that an appropriate Δ value can be set by estimating the frequency spread $\Delta\omega$ of the time-frequency representation. Expression (8) can provide the unbiased estimation as long as the frequency distribution width of the time-frequency representation of SCT can match the parameter Δ value.

3. Analytical signal analysis

To investigate the effectiveness and robustness of the proposed LMSSSCT method, this section constructs analytical signals with different levels of noise. The index of accuracy and Rényi entropy are introduced and calculated to measure energy aggregation and robustness against noise of TFA results. The newly introduced TFA method is compared and validated with several traditional methods such as SST and SET. Among them, SST, SET are all post-processing methods based on short-time Fourier transform.

3.1 Single component signal

A frequency modulated and amplitude modulated analytical single component signal S_1 is established for numerical simulation. The signal is expressed as follows

$$S_1 = e^{-0.15t}\,sin(\,2\pi(50t + 3\,sin(\,3\pi t))) \tag{9}$$

The sampling frequency and sampling time of this signal are 300 Hz and 5 s, respectively. According to Expression (9), the original signal S_1 and its theoretical IF ridge are plotted, respectively, in Figs. 1(a)-(b).

The signal is processed by SST, SET, SCT and LMSSSCT, respectively, and the corresponding time-frequency results are shown in Fig. 2. In this figure, Fig. 2(A)-(a) represent time-frequency representation of SST and corresponding zoom of SST, respectively. The time-frequency representation and its zoom generated by SET are shown in Fig. 2(B)-(b). It is clear that the energy of time-frequency representations processed by SST and SET are both concentrated within a certain bandwidth, but the results also suffer from smeared effect and poor resolution.

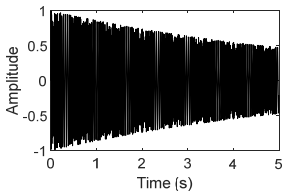

(a) Signal

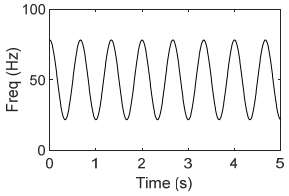

(b) IF

Fig. 1 The original signal S_1 and its theoretical IF

Similarly, Fig. 2(C)-(c) represent SCT and zoom of SCT, respectively. After introducing nonlinear spline interpolated kernel function, it can be observed that the energy of SCT is more concentrated than that of SST and SET. Furthermore, as a kind of post-processing after SCT, the time-frequency representation of LMSSSCT and its zoom shown in Fig. 2(D)-(d) are more energy-concentrated, indicating that the result of LMSSSCT is closer to the theoretical IF and the processing method is more ideal.

Fig. 3 shows the comparison between theoretical IF and identified IF obtained by SST, SET and LMSSSCT. It can be clearly seen from Fig. 3 that SST, SET and LMSSSCT can all approximately identify IF of the signal, but at the inflection points, the errors between identified results of SST/SET and theoretical values are still a little large. The result of LMSSSCT is comparatively closer to theoretical value and the error is smaller, which indicates that LMSSSCT is feasible in TFA and IF identification.

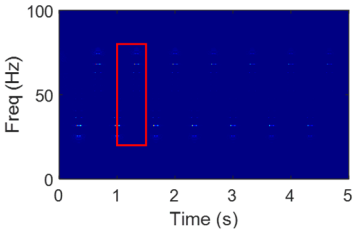

(A) SST

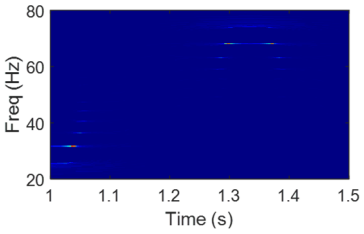

(a) Zoom of SST

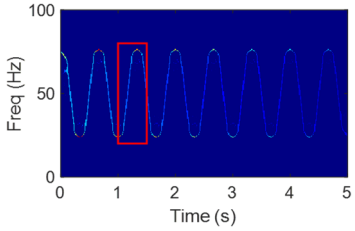

(B) SET

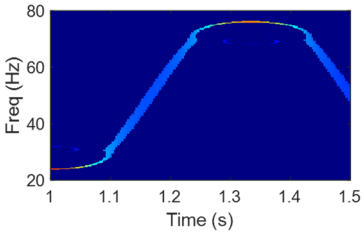

(b) Zoom of SET

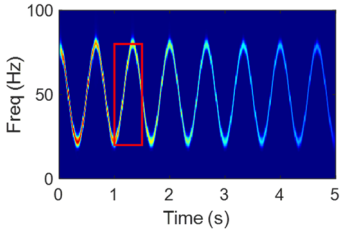

(C) SCT

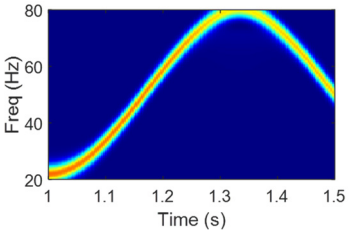

(c) Zoom of SCT

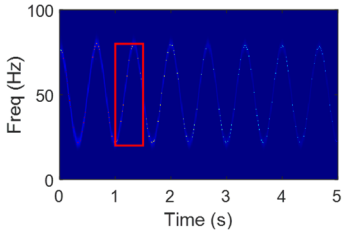

(D) LMSSSCT

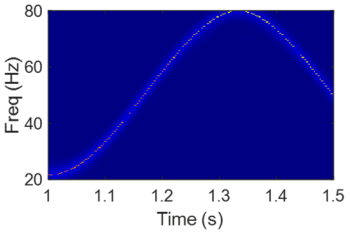

(d) Zoom of LMSSSCT

Fig. 2 Time-frequency representations of signal S_1

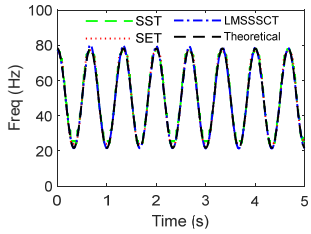

(a) Theoretical IF and identified IF

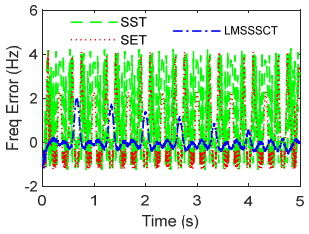

(b) Error between theoretical IF and identified IF

Fig. 3 Comparison of theoretical IF and identified IF of signal S_1

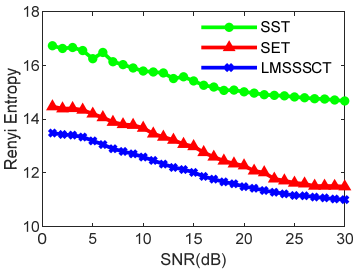

Fig. 4 Rényi entropies of different TFA methods under different levels of noise (SNR = 1~30 dB)

To quantify the accuracy of identified IF compared to theoretical IF, the relative error is introduced by measuring the difference between identified IF and theoretical IF. The relative error is defined as index of accuracy (IA). The calculation method of IA value is expressed by

$$IA = \frac{\sqrt{\int_0^T [f_d(t) - f_e(t)]^2 \mathrm{d}t}}{\sqrt{\int_0^T [f_e(t)]^2 \, \mathrm{d}t}} \times 100\% \tag{10}$$

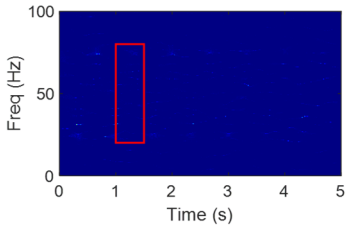

(A) SST

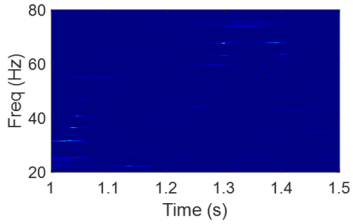

(a) Zoom of SST

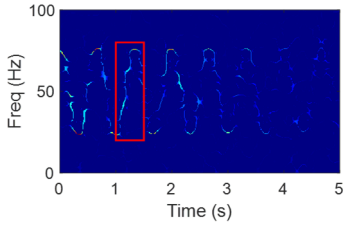

(B) SET

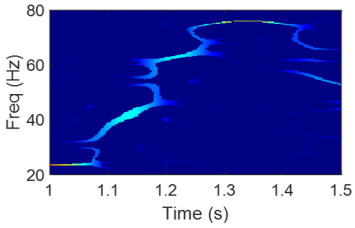

(b) Zoom of SET

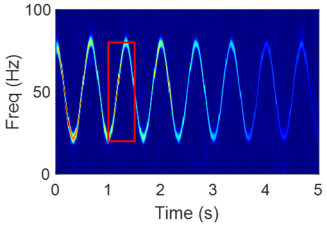

(C) SCT

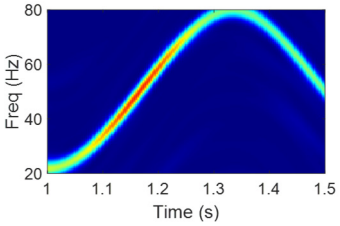

(c) Zoom of SCT

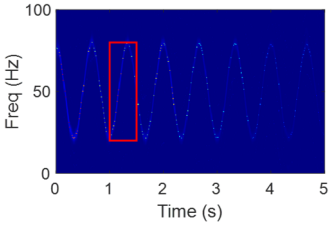

(D) LMSSSCT

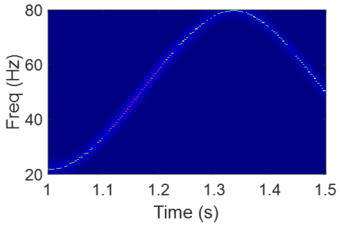

(d) Zoom of LMSSSCT

Fig. 5 Time-frequency representations of S_1 (SNR = 10)

Table 1 The IF identification IA values of signal S_1

Method	SST	SET	LMSSSCT
IA (%)	3.72	2.74	0.81

Table 2 The Rényi entropies of S_1 when SNR = 10 dB and SNR = 25 dB

Method	SST	SET	LMSSSCT
Rényi entropy (10 dB)	15.7964	13.6681	12.5879
Rényi entropy (25 dB)	14.8302	11.6174	11.1503

(a) Signal (b) IF

Fig. 6 The original signal S_2 and its theoretical IF

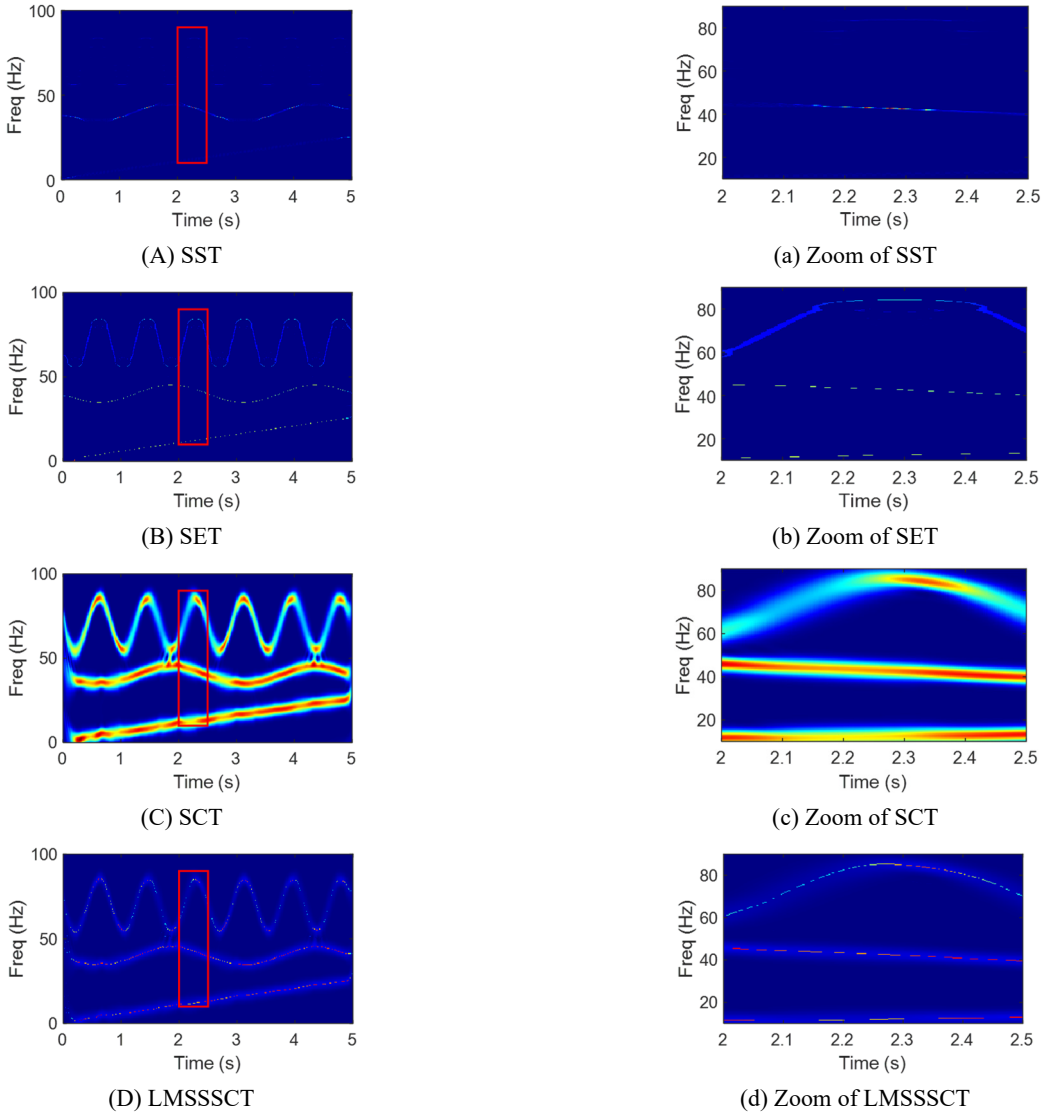

(A) SST (a) Zoom of SST

(B) SET (b) Zoom of SET

(C) SCT (c) Zoom of SCT

(D) LMSSSCT (d) Zoom of LMSSSCT

Fig. 7 Time-frequency representations of S_1

where, $f_d(t)$ is identified IF and $f_e(t)$ represents theoretical IF. The smaller the IA value, the closer the identified IF is to the theoretical IF.

The IA values of SST, SET and LMSSSCT methods are calculated and listed in Table 1. It is obvious that the IA value of LMSSSCT is smaller, which indicates that compared with SST and SET, LMSSSCT has higher accuracy in IF identification and it can be more applicable for signal analysis.

To further study the robustness against noise of this method, different levels of Gaussian white noises (SNR = 1~30 dB) are added to the original signal. The Rényi entropies of time-frequency representations generated by different TFA methods are calculated and shown in Fig. 4. For easy reference, Table 2 lists the Rényi entropies when SNR = 10 dB and SNR = 25 dB. The results (SNR = 10) after processing by different TFA methods are displayed in Fig. 5. According to the Rényi entropies and the time-frequency representations of different methods when SNR = 10, it can be known that LMSSSCT has higher robustness against noise.

3.2 Multi-component signal

To further study the capability of LMSSSCT for analyzing multi-component signals, this paper introduces a multi-component signal including three modes for numerical simulation. The signal is defined is as follows

$$S_2 = \begin{cases} x_1(t) = sin(\,2\pi(t + 2.5t^2)) \\ x_2(t) = sin(\,2\pi(40t + 2.1\,cos(\,0.8\pi t))) \\ x_3(t) = sin(\,2\pi(70t + 2.1\,cos(\,2.4\pi t))) \end{cases} \quad (11)$$

The sampling frequency of this signal is 300 Hz and the sampling time is 5 s. Fig. 6(a) gives the original signal S_2, and Fig. 6(b) shows the theoretical IF trajectory of signal S_2.

The same methods are used to perform TFA of the signal, and the corresponding results are shown in Fig. 7(A)-(a) represent time-frequency representation of SST and corresponding zoom of SST, respectively. Fig. 7(B)-(b) give result of SET and zoom of SET. Similarly, Fig. 7(C)-(c) show result of SCT and zoom of SCT, respectively. By applying local maximum synchrosqueezing to the SCT result, the time-frequency representation of LMSSSCT and its zoom are shown in Fig. 7(D)-(d). It can be observed that the energy concentration of the SCT result is greatly improved by the operation of local maximum synchrosqueezing, and the LMSSSCT behaves better than the SST and SET methods.

Fig. 8 shows the comparison between identified frequency by different methods and theoretical frequency. Table 3 lists the IA values of SST, SET and LMSSSCT. It is obvious that the IA value of LMSSSCT is smaller, which indicates that compared with SST and SET, the identified IF features based on the LMSSSCT result are highly consistent with the theoretical Ifs.

Again, various levels of Gaussian white noises (SNR = 1~30 dB) are added to S_2, and Rényi entropies of time-frequency representations generated by different methods are calculated and displayed in Fig. 9. From Fig. 9, it is obvious that the LMSSSCT results achieve the minimum in each noise level, which denotes that the LMSSSCT has the best ability to improve the time-frequency energy concentration for multi-component signals. Table 4 lists the Rényi entropies measured when SNR = 10 dB and SNR = 25 dB to quantitatively evaluate the energy concentration of different time-frequency results. From Table 4, it can be founded that LMSSSCT shows the most excellent performance in energy concentration among these TFA methods. Fig. 10 shows the time-frequency representations processed by these different TFA methods when SNR = 10 dB. As can be seen from Fig. 10 that the performance of

Table 3 The IF identification IA values of signal S_2

Method	SST	SET	LMSSSCT
IA_1 (%)	1.85	4.21	1.53
IA_2 (%)	1.27	1.60	0.84
IA_3 (%)	1.85	1.82	0.67

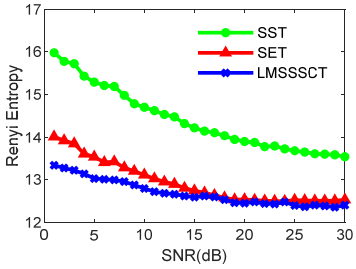

Fig. 9 Rényi entropies of different TFA methods under different levels of noise (SNR = 1~30 dB)

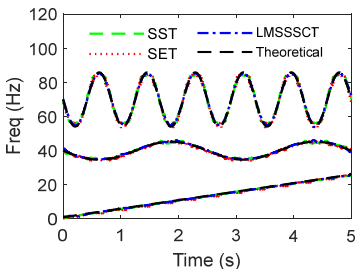

(a) Theoretical IF and identified IF

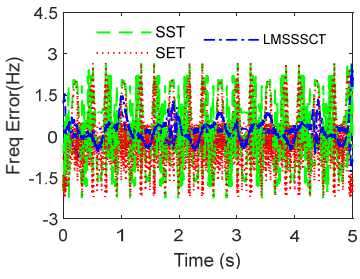

(b) Error between theoretical IF and identified IF

Fig. 8 Comparison of theoretical IF and identified IF of signal S_2

SST is unsatisfactory. The performance of SET is poor for the 3rd component, however, good for the first two modes. For LMSSSCT, it has the highest energy concentration with the lowest Rényi entropies.

4. Structural simulation

4.1 Duffing nonlinear system

To further study the ability of LMSSSCT to analyze and process single-degree-of-freedom structural non-stationary vibration signal, the classical Duffing system is introduced to simulate a nonlinear structural system, and the free vibration equation of the nonlinear system is

$$\ddot{y} + 0.05\dot{y} + y + 0.2y^3 = 0 \tag{12}$$

where, initial conditions are set as: $y_0 = 10$, $\dot{y} = 0$. The fourth-order Runge-Kutta method is used to solve the displacement response. The duration and interval are $t = 100\,s$ and $\Delta t = 0.1\,s$, respectively. The displacement response of the nonlinear structural system is shown in Fig. 11.

Table 4 The Rényi entropies of S_2 when SNR = 10 dB and SNR = 25 dB

Method	SST	SET	LMSSSCT
Rényi entropy (10 dB)	14.6989	13.1135	12.7952
Rényi entropy (25 dB)	13.6802	12.5207	12.3949

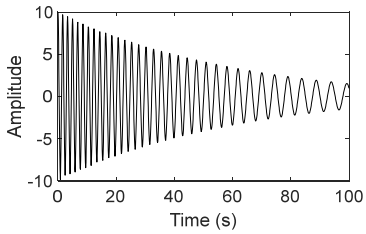

Fig. 11 Displacement response of duffing system

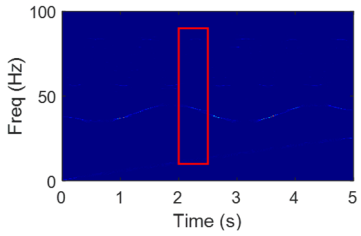

(A) SST

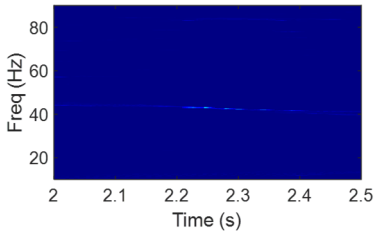

(a) Zoom of SST

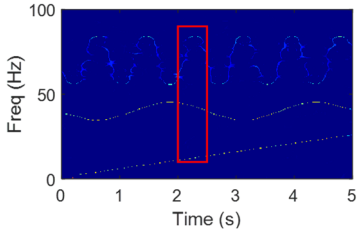

(B) SET

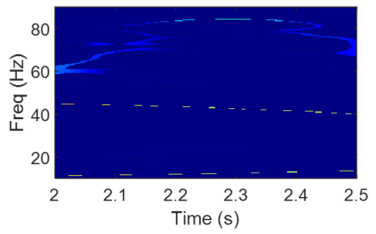

(b) Zoom of SET

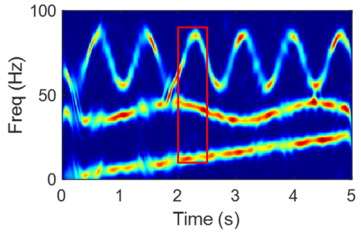

(C) SCT

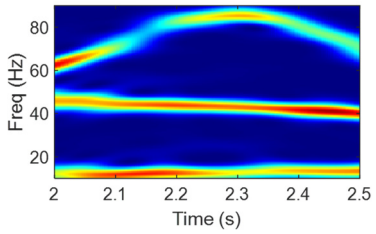

(c) Zoom of SCT

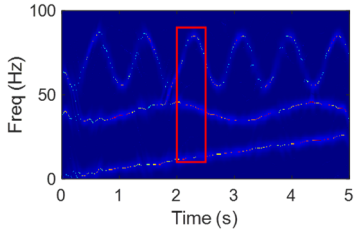

(D) LMSSSCT

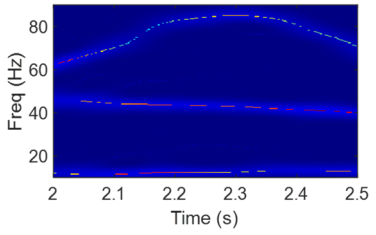

(d) Zoom of LMSSSCT

Fig. 10 Time-frequency representations of S_2 (SNR = 10)

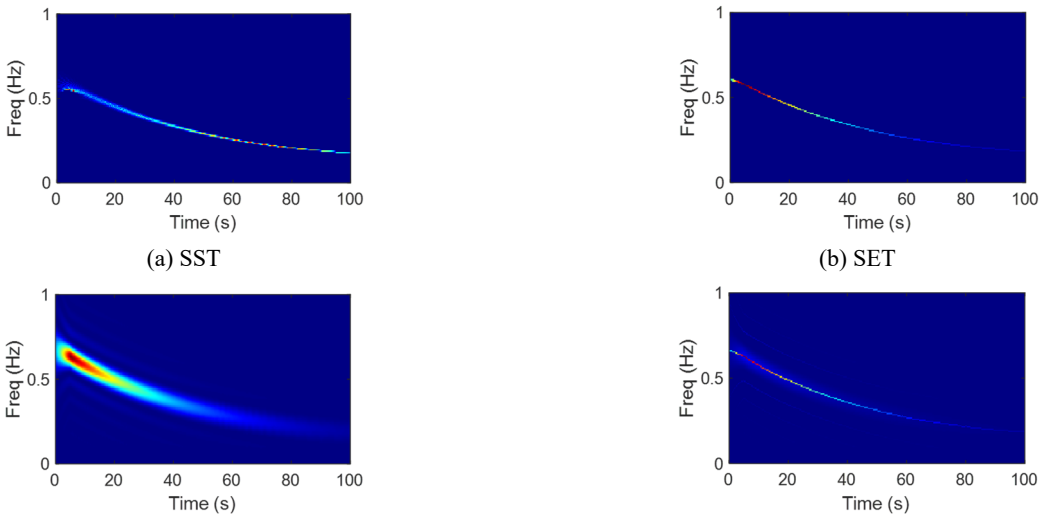

(a) SST (b) SET

(c) SCT (d) LMSSSCT

Fig. 12 Time-frequency diagram of displacement response of duffing system

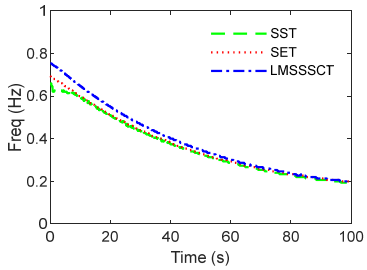

Fig. 13 IF of displacement response of duffing system

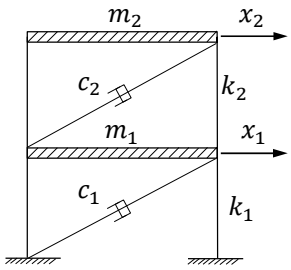

Fig. 14 Two-layer shear frame structure

The TFA of the Duffing system displacement response is performed by using SST, SET and LMSSSCT respectively, and the results are shown in Fig. 12. It can be seen from this figure that due to the large displacement, strong energy, and high degree of nonlinearity in the initial stage, the IF gradually decreased from 0.66 Hz. With the weakening of structural response and energy, the change of frequency ridge is gradually flattened, and finally tends to be stable around 0.18 Hz. The IF trends of SST, SET and LMSSSCT are basically the same, but the burr phenomenon appears in the initial vibration stage of SST and SET, and the aggregation of time-frequency representation is not as good as that of LMSSSCT.

The extracted IF of Duffing system is displayed in Fig. 13. SST fluctuates greatly at the beginning points and the burr phenomenon is more severe, so it cannot effectively identify the initial frequency. There are some differences between SET and LMSSSCT at the beginning points. Using the equivalent stiffness method, the initial frequency can be approximately calculated to be 0.64 Hz, and the identified results of SET and LMSSSCT are 0.61 Hz and 0.66 Hz, respectively, with comparable accuracy. Overall, the processing results of SET and LMSSSCT are more ideal than that of SST.

Table 5 Parameters of two-layer shear frame structure

Layer	Quality m/kg	Damping coefficient $c/(N \cdot s \cdot m^{-1})$	Initial stiffness $k/(N \cdot m^{-1})$
First	5.85×10^5	2.08×10^5	2.15×10^8
Second	4.95×10^5	1.15×10^5	0.95×10^8

4.2 Two-layer frame structure

4.2.1 Time-varying stiffness frame

To verify the feasibility of the proposed method for IF identification of multi-degree-of-freedom system, a two-layer time-varying stiffness frame model shown in Fig. 14 is used for numerical simulation and verification, and the physical parameters of the structure are shown in Table 5.

The dynamic equation of the frame structure is

$$\begin{cases} m_1\ddot{y}_1 + (c_1 + c_2)\dot{y}_1 - c_2\dot{y}_2 + (k_1 + k_2)y_1 - k_2y_2 \\ \qquad\qquad = f_1 \\ m_2\ddot{y}_2 - c_2\dot{y}_1 + c_2\dot{y}_2 - k_2y_1 + k_2y_2 = f_2 \end{cases} \tag{13}$$

where, the time-varying stiffness k_1 and k_2 meet the following conditions

$$k_1 = \begin{cases} 2.15 \times 10^8, & 0 \le t < 4 \\ \{2.15 - 0.06 \times (t-4) \\ \quad -0.1 \times sin[\frac{\pi}{2}(t-4)]\} \times 10^8, & 4 \le t < 16 \\ 1.43 \times 10^8, & 16 \le t < 25 \end{cases} \quad (14)$$

$$k_2 = \begin{cases} 0.95 \times 10^8, & 0 \le t < 4 \\ [0.95 - 0.15 \times (t-4)] \times 10^8, & 4 \le t < 8 \\ 0.35 \times 10^8, & 8 \le t < 25 \end{cases} \quad (15)$$

The curve of time-varying stiffness is shown in Fig. 15(a). By calculating matrix eigenvalues, the theoretical IF trajectory of the frame structure can be obtained and shown in Fig. 15(b).

4.2.2 White noise excitation

Gaussian white noise is firstly used to excite the frame structure, and the white noise excitation is shown in Fig. 16(a). The dynamic response of the frame structure is solved by Runge-Kutta method, and the displacement response of the first layer is shown in Fig. 16(b). The sampling frequency is 50 Hz and the sampling time is 25 s.

TFA of displacement response signal of the first layer under white noise excitation is performed by SST, SET and LMSSSCT, and the calculation time-frequency results are shown in Fig. 17. It can be seen from this figure that the low-order frequency energy aggregation of SST is good, but the high-order frequency energy aggregation is not obvious. So, the identified high-order IF ridge is not ideal. For SET, time-frequency energies of both two orders frequency are

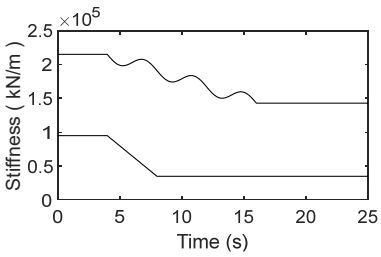

(a) Stiffness

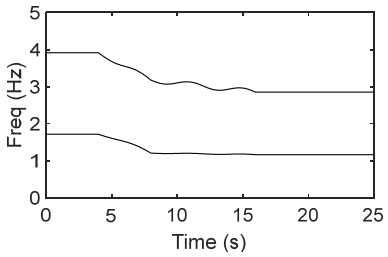

(b) IF

Fig. 15 Stiffness and theoretical IF of frame structure

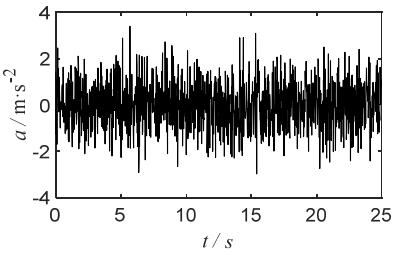

(a) Excitation

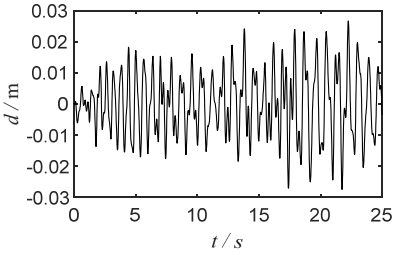

(b) Response

Fig. 16 White noise excitation and displacement response of the first layer

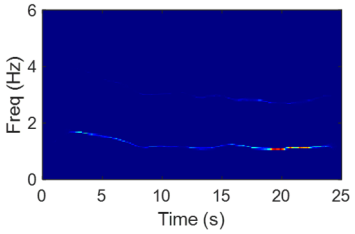

(a) SST

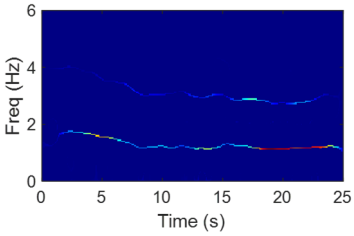

(b) SET

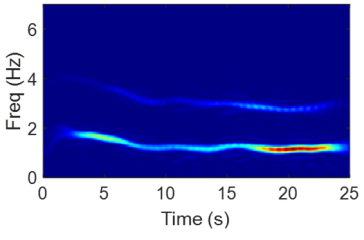

(c) SCT

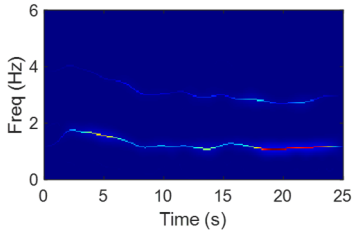

(d) LMSSSCT

Fig. 17 Time-frequency representations under white noise excitation

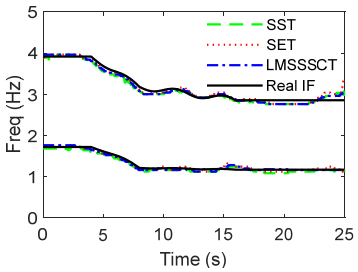

(a) Theoretical IF and identified IF

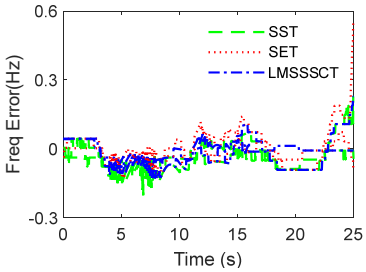

(b) Error between theoretical IF and identified IF

Fig. 18 Identified IF under white noise excitation

Table 6 The IF identification IA values of signal under white noise excitation

Method	SST	SET	LMSSSCT
IA_1 (%)	4.16	3.17	3.00
IA_3 (%)	2.42	2.56	2.18

relatively concentrated. The energy concentration of SCT is greatly improved by local maximum synchrosqueezing, and the LMSSSCT behaves better than the SST method.

The IF of the structure can be roughly identified by the three methods, and the recognized IF is shown in Fig. 18. The frequency recognized by SST has a large local fluctuation and the burr phenomenon is more serious. Affected by short-time Fourier transform, the IF identified by SET deviates slightly at the ending points. The fluctuation and end deviation of LMSSSCT results are relatively smaller, which indicates that it has high accuracy in IF identification.

4.2.3 Earthquake excitation

The 1940 EL-Centro earthquake wave is further used to excite the frame structure. The displacement, velocity and acceleration responses of the structure are obtained by using Runge-Kutta method. The sampling frequency is 50 Hz and

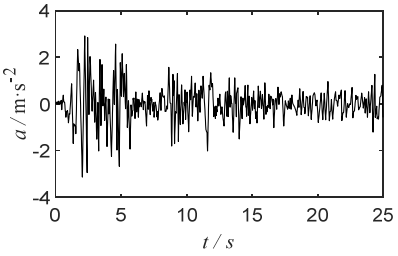

(a) Excitation

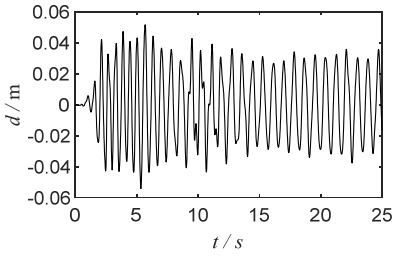

(b) Response

Fig. 19 EL-Centro earthquake excitation and displacement response of the first layer

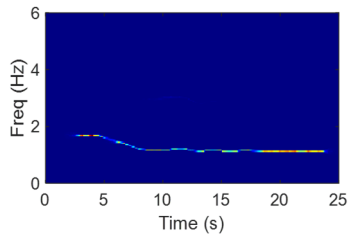

(a) SST

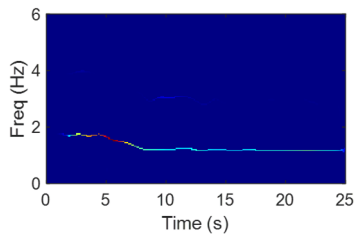

(b) SET

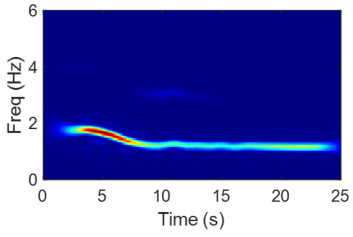

(c) SCT

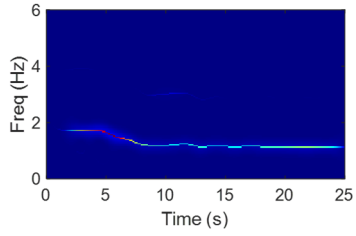

(d) LMSSSCT

Fig. 20 Time-frequency diagram under EL-Centro earthquake excitation

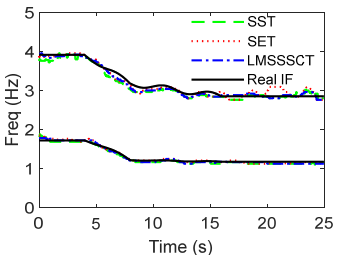

(a) Theoretical IF and identified IF

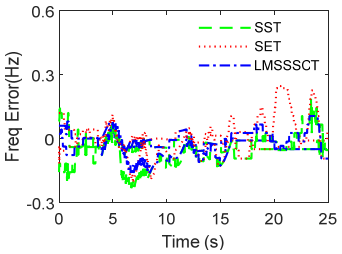

(b) Error between theoretical IF and identified IF

Fig. 21 Identified frequency under EL-Centro earthquake excitation

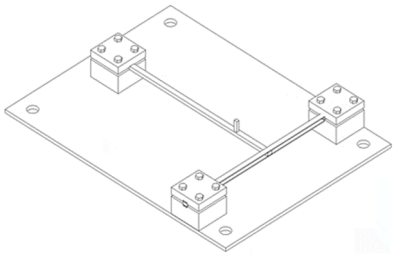

(a) Structure

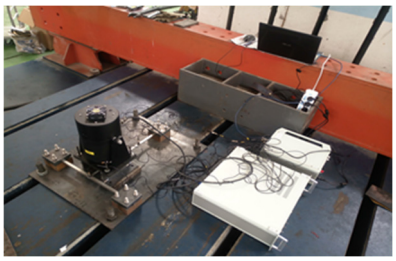

(b) Device

Fig. 22 Test structure and device

Table 7 The IF identification IA values of signal under EL-Centro earthquake excitation

Method	SST	SET	LMSSSCT
IA_1 (%)	3.19	2.61	2.52
IA_3 (%)	3.04	3.03	2.18

the sampling time is 25 s.

SST, SET, and LMSSSCT are again used to carry out TFA of the first layer displacement response signal, and the time-frequency results are shown in Fig. 20. The recognized IF is displayed in Fig. 21. It can be seen from Fig. 20 that the energy of the response signal under earthquake excitation is mainly concentrated in the low-order frequency, and the high-order frequency energy is relatively small. The time-frequency ridge of LMSSSCT is slightly smoother than that of SST and SET. From Fig. 21, we can know that the frequency burr phenomenon identified by SST is more serious. The high-order IF recognized by SET has a slightly larger deviation in local position (20 s to 25 s). The LMSSSCT result has relatively better smoothness and smaller ending deviation. To sum up, the LMSSSCT is also able to perform IF identification of multi-degree freedom structures with varying stiffness, and the results are relatively accurate.

5. Experimental verification

5.1 Nonlinear supported beam structure

To further verify the IF identification accuracy of LMSSSCT algorithm in actual nonlinear structure, a rectangular cross-section nonlinear supported beam structure is designed for experimental verification. As shown in Fig. 22(a), one end of the beam is fixed and the other end is clamped with two identical sheets to simulate the nonlinear spring support. The rectangular beam is 500 mm long and the cross-section size is 15 mm × 10 mm. The section size of the sheet is 15 mm × 2 mm. The material density is 7930 kg/m^3, and the elastic modulus is 1.93 × 10^5 MPa. The excitation point is 380 mm far away from the fixed end, and the acceleration sensor is set at the flake support end. Layout of the test device is shown in Fig. 22(b).

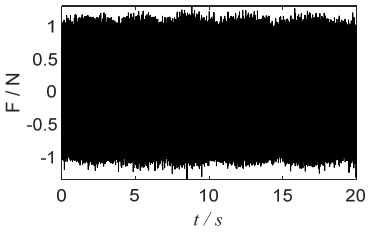

(a) Excitation

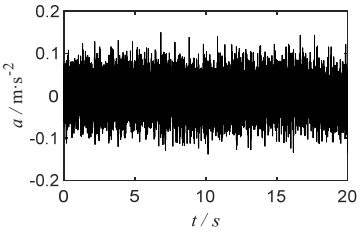

(b) Response

Fig. 23 White noise excitation and acceleration response

5.2 Low amplitude white noise excitation

To obtain the natural frequency, the beam structure is first excited by low amplitude white noise and the acceleration response is collected. Then, the natural frequency of the structure is approximatively obtained by fast Fourier transform (FFT). The low amplitude white noise excitation is shown in Fig. 23(a) and the acceleration response signal is shown in Fig. 23(b). The FFT result is shown in Fig. 24, and the natural frequency of the structure obtained by FFT is about 50.05 Hz.

After obtaining the natural frequency, acceleration response signal acquired in the subsequent test is resampled and preprocessed, and the filter is used to remove the components above the second-order frequency. Finally, the preprocessed signal is analyzed by TFA methods. Through comparison of various methods, the ability of LMSSSCT to identify structural IF is verified.

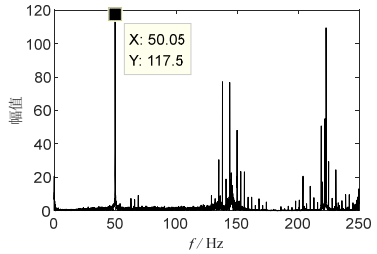

Fig. 24 Spectrum of FFT

5.3 Random load excitation

To explore IF characteristics of the beam structure during nonlinear vibration, a random load with higher amplitude is used to excite the structure. Acceleration response signal of the structure is collected, and the TFA methods are used to analyze and identify IF. The random load excitation is shown in Fig. 25(a) and the collected acceleration response is shown in Fig. 25(b).

Similarly, SST, SET and LMSSSCT are used to analyze the acceleration response signal, and the obtained time-frequency results are shown in Fig. 26. The IFs identified by TFA are shown in Fig. 27. As can be seen from Fig. 26, the SST result is approximately a straight line, and its non-stationary instantaneous characteristics cannot be identified. The time-varying characteristic of IF ridge is also not obvious in SET. The IF trajectory of LMSSSCT fluctuates up and down with time in a certain range, which reflects the time-varying characteristics of the nonlinear structural vibration response signal under random load. From Fig. 27, it can be known that the IF identified by SST, SET and LMSSSCT change little over time, but the frequency curve recognized by LMSSSCT can better reflect the time-varying characteristics.

(a) Excitation (b) Response

Fig. 25 Random load excitation and acceleration response

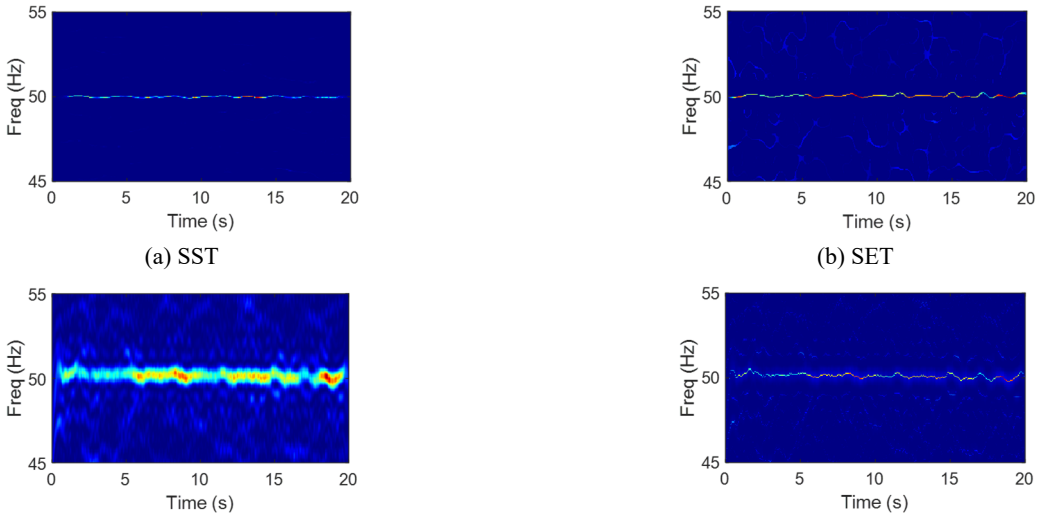

(a) SST (b) SET

(c) SCT (d) LMSSSCT

Fig. 26 Time-frequency diagram under random load excitation

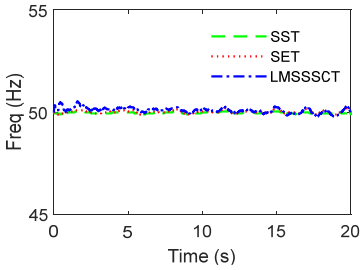

Fig. 27 Identified frequency under random load excitation

6. Conclusions

The vibration responses of practical engineering structures are generally non-stationary. To further improve energy aggregation of non-stationary signals, in this paper, the LMSSSCT method has been proposed based on the chirplet transform with spline interpolated kernel function and the local maximum synchrosqueezing. The superior accuracy and robustness against noise of this method are verified by IF identifications of both single component signal and multi-component signal with different levels of noise. In terms of numerical structural simulation, a nonlinear Duffing system and a two-layer time-varying stiffness shear frame model are used respectively to verify the effectiveness of the proposed method. Furthermore, a nonlinear supported beam structure test is designed and carried out to validate the effectiveness of this method for practical structures. The IF identified by LMSSSCT is compared with the IFs identified by SST, SET and theoretical frequency to verify the effectiveness and superiority of the proposed method.

Based on the results, it can be concluded that:

- By introducing spline interpolated function as kernel function, the spline chirplet transform can effectively perform TFA of nonlinear frequency modulated signals. Taking the advantages of SCT and local maximum synchrosqueezing, LMSSSCT can greatly improve the energy concentration in time-frequency domain, and clearly identify the IF.
- Numerical simulation results indicate that the proposed LMSSSCT method has higher accuracy and better robustness against noise than SST and SET methods when processing single component and multi-component analytic signals.
- Structural simulation and experimental results show that the LMSSSCT method can effectively identify IF of nonlinear and time-varying structures with high accuracy and good stability.

Acknowledgments

Financial support to complete this study is provided in part by the National Natural Science Foundation of China (Grant No. 51979130), Natural Science Foundation of Jiangsu Province (Grant No. BK20191460), Natural Science Research of Jiangsu Higher Education Institutions of China (Grant No. 20KJB560016) and Postdoctoral Research Funding Program of Jiangsu Province (Grant No. 2021K562C). The results and opinions expressed in this paper are those of the authors only and they don't necessarily represent those of the sponsors.

References

Chen, H., Lu, L., Xu, D., Kang, J. and Chen, X. (2017), "The synchrosqueezing algorithm based on generalized S-transform for high-precision time-frequency analysis", *Appl. Sci.*, **7**, 769. https://doi.org/10.3390/app7080769

Chen, P., Wang, K., Zuo, MJ. and Wei, D. (2019), "An ameliorated synchroextracting transform based on upgraded local instantaneous frequency approximation", *Measurement*, **148**, 106953. https://doi.org/10.1016/j.measurement.2019.106953

Daubechies, I., Lu, J.F. and Wu, H.T. (2011), "Synchrosqueezed wavelet transforms: An empirical mode decomposition-like tool", *Appl. Comput. Harmon. A*, **30**(2), 243-261. https://doi.org/10.1016/j.acha.2010.08.002

Guan, Y. and Feng, Z. (2022), "Adaptive linear chirplet transform for analyzing signals with crossing frequency trajectories", *IEEE Trans. Ind. Electron.*, **69**(8), 8396-8410. https://doi.org/10.1109/TIE.2021.3097605

Guan, Y., Liang, M. and Necsulescu, D.S. (2019), "Velocity synchronous linear chirplet transform", *IEEE Trans. Ind. Electron.*, **66**(8), 6270-6280. https://doi.org/10.1109/TIE.2018.2873520

He, Y., Jiang, Z., Hu, M. and Li, Y. (2021), "Local maximum synchrosqueezing chirplet transform: An effective tool for strongly nonstationary signals of gas turbine", *IEEE T. Instrum. Meas.*, **70**, 1-14. https://doi.org/10.1109/TIM.2021.3076588

Li, Z., Gao, J., Li, H., Zhang, Z., Liu, N. and Zhu, X. (2020a), "Synchroextracting transform: The theory analysis and comparisons with the synchrosqueezing transform", *Signal Process.*, **166**, 107243. https://doi.org/10.1016/j.sigpro.2019.107243

Li, M.F., Wang, T.Y., Chu, F.L., Han, Q.K., Qin, Z.Y. and Zuo, MJ. (2020b), "Scaling-basis chirplet transform", *IEEE Trans. Ind. Electron.*, **68**(9), 8777-8788. https://doi.org/10.1109/TIE.2020.3013537

Liu, H. and Xiang, J. (2018), "Kernel regression residual decomposition-based synchroextracting transform to detect faults in mechanical systems", *ISA. Trans.*, **87**, 251-263. https://doi.org/10.1016/j.isatra.2018.12.004

Liu, J.L., Zheng, J.Y., Wei, X.J., Liao, F.Y. and Luo, Y.P. (2018a), "A new instantaneous frequency extraction method for nonstationary response signals in civil engineering structures", *J. Low Freq. Noise Vib. Active Control*, **37**(4), 834-848. https://doi.org/10.1177/1461348418790534

Liu, J.L., Wei, X.J., Qiu, R.H., Zheng, J.Y., Zhu, Y.J. and Laory, I. (2018b), "Instantaneous frequency extraction in time-varying structures using a maximum gradient method", *Smart Struct. Syst., Int. J.*, **22**(3), 359-368. https://doi.org/10.12989/sss.2018.22.3.359

Liu, J.L., Zheng, J.Y., Wei, X.J., Ren, W.X. and Laory, I. (2019), "A combined method for instantaneous frequency identification in low frequency structures", *Eng. Struct.*, **194**, 370-383. https://doi.org/10.1016/j.engstruct.2019.05.057

Meng, Z., Lv, M., Liu, Z. and Fan, F. (2021), "General synchroextracting chirplet transform: Application to the rotor rub-impact fault diagnosis", *Measurement*, **169**, 108523. https://doi.org/10.1016/j.measurement.2020.108523

Pham, D.H. and Meignen, S. (2017), "High-order synchro-squeezing transform for multicomponent signals analysis-with

an application to gravitational gravitational-wave signal", *IEEE T. Signal Process*., **65**(12), 3168-3177. https://doi.org/10.1109/TSP.2017.2686355

Sahu, G., Dash, S. and Biswal, B. (2020), "Time-frequency analysis of power quality disturbances using synchroextracting transform", *Int. T. Electr. Energy*, **30**(4), e12278. https://doi.org/10.1002/2050-7038.12278

Shi, Z., Yang, X., Li, Y. and Yu, G. (2021), "Wavelet-based synchroextracting transform: An effective TFA tool for machinery fault diagnosis", *Control Eng. Pract*., **114**(5), 104884. https://doi.org/10.1016/j.conengprac.2021.104884

Sony, S. and Sadhu, A. (2020), "Synchrosqueezing transform-based identification of time-varying structural systems using multi-sensor data", *J. Sound Vib*., **486**, 115576. https://doi.org/10.1016/j.jsv.2020.115576

Wang, Z.C., Ren, W.X. and Liu, J.L. (2013), "A synchrosqueezed wavelet transform enhanced by extended analytical mode decomposition method for dynamic signal reconstruction", *J. Sound Vib*., **332**(22), 6016-6028. https://doi.org/10.1016/j.jsv.2013.04.026

Wang, C., Zhang, J. and Zhu, H.P. (2020), "A combined method for time-varying parameter identification based on variational mode decomposition and generalized Morse wavelet", *Int. J. Struct. Stab. Dyn*., **20**(7), 1-24. https://doi.org/10.1142/S0219455420500777

Xin, Y., Hao, H. and Li, J. (2019), "Time-varying system identification by enhanced empirical wavelet transform based on synchroextracting transform", *Eng. Struct*., **196**, 109313. https://doi.org/10.1016/j.engstruct.2019.109313

Yang, Y., Peng, Z.K., Meng, G. and Zhang, W.M. (2011), "Spline-kernelled chirplet transform for the analysis of signals with time-varying frequency and its application", *IEEE Trans. Ind. Electron*., **59**(3), 1612-1621. https://doi.org/10.1109/TIE.2011.2163376

Yang, Y., Zhang, W., Peng, Z. and Meng, G. (2013), "Multicomponent signal analysis based on polynomial chirplet transform", *IEEE Trans. Ind. Electron*., **60**(9), 3948-3956. https://doi.org/10.1109/TIE.2012.2206331

Yang, Y., Peng, Z.K., Dong, X.J., Zhang, W.M. and Meng, G. (2014), "General parameterized time-frequency transform", *IEEE Trans. Signal Process*., **62**(11), 2751-2764. https://doi.org/10.1109/TSP.2014.2314061

Yu, G. and Zhou, Y. (2016), "General linear chirplet transform", *Mech. Syst. Signal Pr*., **70-71**, 958-973. https://doi.org/10.1016/j.ymssp.2015.09.004

Yu, G., Yu, M. and Xu, C. (2017), "Synchroextracting transform", *IEEE Trans. Ind. Electron*., **64**(10), 8042-8054. https://doi.org/10.1109/TIE.2017.2696503

Yu, G., Wang, Z. and Zhao, P. (2018), "Multisynchrosqueezing transform", *IEEE Trans. Ind. Electron*., **66**(7), 5441-5455. https://doi.org/10.1109/TIE.2018.2868296

Yu, G., Wang, Z., Zhao, P. and Li, Z. (2019), "Local maximum synchrosqueezing transform: An energy-concentrated time-frequency analysis tool", *Mech. Syst. Signal Pr*., **117**, 537-552. https://doi.org/10.1016/j.ymssp.2018.08.006

Yuan, P.P., Cheng, X.L., Wang, H.H., Zhang, J., Shen, Z.X. and Ren, W.X. (2021), "Structural instantaneous frequency extraction based on improved multi-synchrosqueezing generalized S-transform", *Smart Struct. Syst*., *Int. J*., **28**(5), 675-687. https://doi.org/10.12989/sss.2021.28.5.675

Yuan, P.P., Zhang, J., Feng, J.Q., Wang, H.H., Ren, W.X. and Wang, C. (2022), "An improved time-frequency analysis method for structural instantaneous frequency identification based on generalized S-transform and synchroextracting transform", *Eng. Struct*., **252**, 113657. https://doi.org/10.1016/j.engstruct.2021.113657

Zhu, X., Zhang, Z., Gao, J., Li, B. and Wen, G. (2019), "Synchroextracting chirplet transform for accurate IF estimate and perfect signal reconstruction", *Digit. Signal Process*., **93**, 172-186. https://doi.org/10.1016/j.dsp.2019.07.015